Using Bayesian inference and novel clustering and age dating techniques, we obtain a robust estimate for disk decay lifetimes of 5.8 Myr.

Fabian A. Polnitzky[1], Sebastian Ratzenböck[2], Josefa Großschedl[3], João Alves[1]

[1]University of Vienna, [2]Center for Astrophysics, [3]Astronomical Institute of the Czech Academy of Sciences

Precise determination of circumstellar disk lifetimes: Disk evolution in a single star-forming region

Background

Having an accurate estimate of the **lifetimes of circumstellar disks** around Young Stellar Objects (YSOs) also constrains the timescales for planet formation. Previous studies on the evolution of the disk fraction in stellar cluster versus their age use exponential decay models and obtain decay times of 2-3 Myr [F10, R14, R15, R18], but also larger estimates of 8 Myr are reported [M21]. For these types of studies, one needs precise information on the membership of stellar sources to stellar clusters and a homogeneous determination of stellar cluster ages. In this work, we use recent results to mitigate both problems. In [R23a], the authors developed a novel clustering algorithm, SigMA, and apply this to the **Scorpius-Centaurus OB association** using positional and velocity data from *Gaia* DR3 [GC21]. In a subsequent work, [R23b] determine the isochronal ages for the stellar clusters in the *Gaia* color-magnitude diagrams. We take the 33 stellar clusters, that comprise this star-forming region, spanning ages from 3 to 21 Myr. However, there are also some biases that we cannot remove. [P22] argue that combining stellar clusters at different distances lead to an overrepresentation of high mass stars, also the disk lifetime is influenced by the central stellar mass [e.g. R15].

Methods

We start from the 33 stellar clusters with PARSEC **isochronal ages** from [R23b], comprising more than 10000 stellar sources and first determine the presence or absence of circumstellar disks. As circumstellar disks are detected in infrared, we use photometric measurements from WISE and 2MASS for this. We use three approaches and compare their results among each other. First, we use **color-color diagrams** (CCD selection) to separate the groups of disk-bearing and disk-less stellar sources [e.g. KL14]. We use four different combinations of colors from WISE and 2MASS to obtain a flexible determination of disks. Next, we perform a linear fit to the **spectral energy distribution** (SED selection) in the infrared and use the slope as indicator of infrared excess [G19]. Lastly, a **recent paper** ([L22]) determines the disk types in the Scorpius-Centaurus OB association, which we take as additional disk selection method (Luhman selection).

We use all three methods to determine the disk fractions for each stellar cluster. As a relation between the disk fraction and stellar cluster age, we use an exponential function of the form $f(t) = f_0 \cdot e^{-\frac{t-t_0}{\tau}}$. The parameters are the **disk decay time** τ, the **initial disk fraction** f_0 and the **shift** t_0. The introduction of t_0 shifts the function along the x-axis to the right, so that it only covers the data range of 3 to 21 Myr. Additionally, this helps alleviate the degeneracy between the decay time and the initial disk fraction. We use Bayesian inference to obtain posterior probability distribution functions (PDFs) for all three parameters. For this, three different models are constructed, which differ in their choices and limits for the prior PDFs. The **fiducial model** constrains the parameters to their physical values, for example the initial disk fraction can only lie between 0 and 1. The **data-driven model** is not constrained to these physical values and the parameters can take any values that describe the data. The **no-shift model** fits the standard exponential without the shift t_0 and the two parameters (disk decay time and initial disk fraction) are not constrained to their physical values.

Results & Conclusions

The different models and disk selection methods are fitted to the data and posterior PDFs are obtained for the parameters. These are shown in **Fig. 1** for the disk decay time. No difference in the models are observed, while the result depends on the disk selection method. These differences are explained in **Fig. 2**, where the disk fractions versus age are shown with their inference results. The median of the fiducial model and the CCD disk selection is **5.8 Myr**.

These results are larger than the estimates obtained in the literature. This is because our work uses for the first time **one coherent star-forming region** with the same initial conditions for the star formation process, but our data is also homogeneous in the clustering algorithm and age dating method. These help to resolve some biases, but not all. Our results still depend on the stellar mass of the central object, which ranges from the hydrogen burning limit up to 8 solar masses and marginalizes over the Gaia selection function at 100-200 pc.

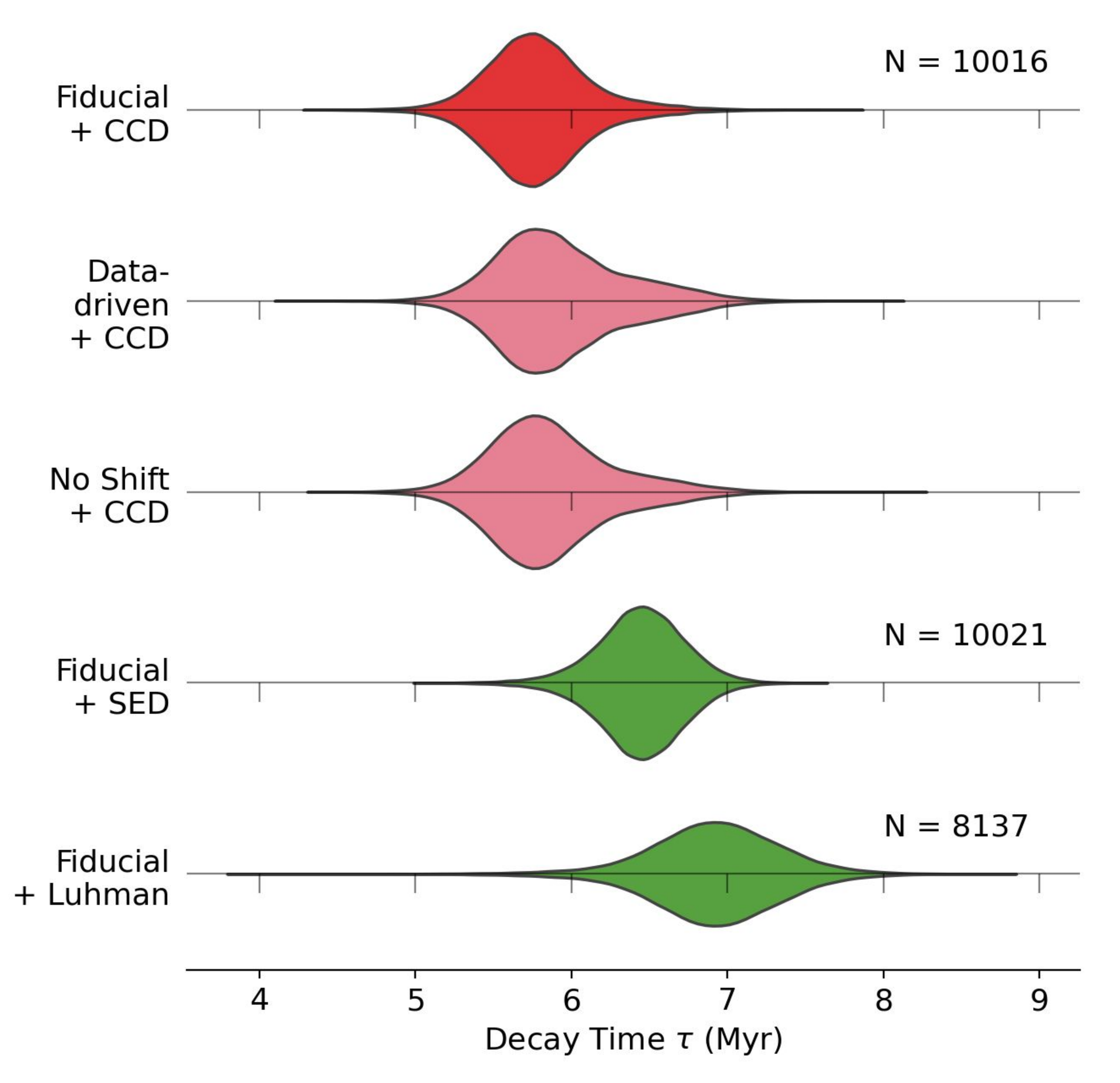

Fig. 1. Posterior PDFs of the disk decay time τ for the three different models (red and pink) and different disk detection methods (green). N gives the number of stellar sources used in each inference. The exact combination of model and disk selection method is listed on the left. Overall all results yield larger disk decay times than previous literature estimates (see left text) with the median result of the fiducial model and the CCD selection at 5.8 Myr. The red and pink posterior distributions show that the choice of prior PDFs in the modeling do not influence the resulting disk decay time, which gives a robust estimate. However, the initial disk fraction and shift differ. Changing the disk selection method shifts the disk decay time to even larger values. The largest is given by the disks of [L22], where the increase in uncertainty is because of a reduced number of stellar sources as this study considers a smaller region as [R23a]. See also below for the implications of this.

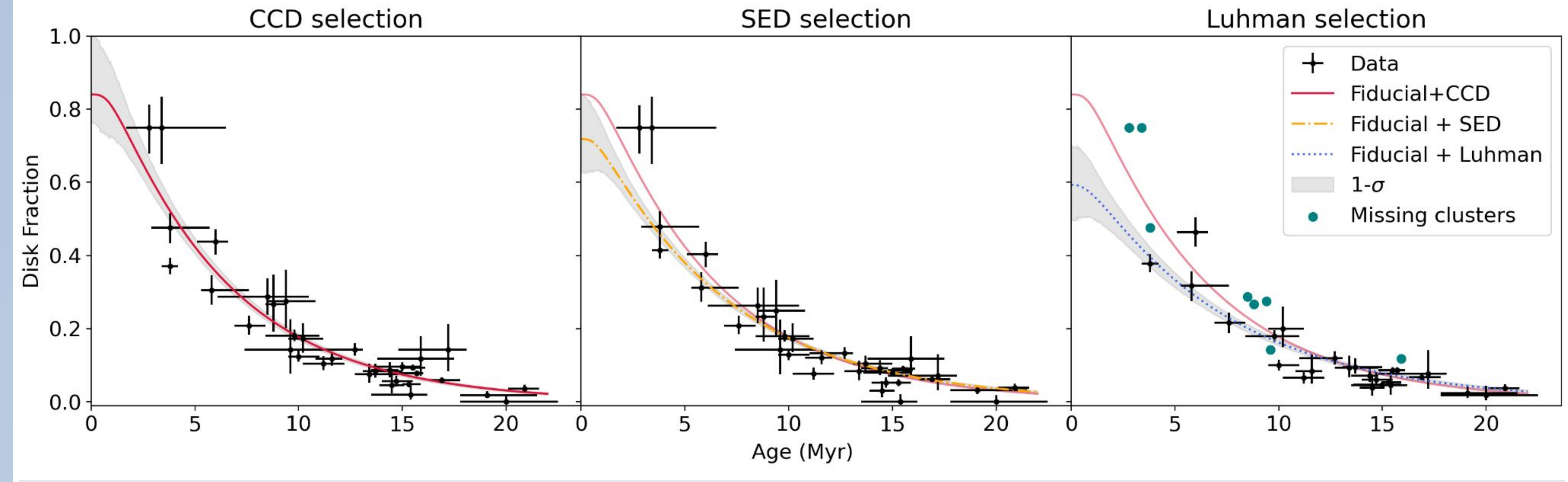

Fig. 2. Disk fraction versus stellar cluster age relation with inference results. The age and uncertainties are taken from [R23b], while the title gives the method used to derive the disk fractions. The uncertainty in disk fraction is modelled from the likelihood. The lines and grey area give the median result and standard deviation of the fiducial model for each disk selection method. The fiducial model + CCD selection result (red line) is visible in all three plots and shows that above 10 Myr the results of the disk selection methods overlap and differences stem from the degeneracy of initial disk fraction and disk decay time. Difference in the results when using the disks from [L22] is because 8 stellar clusters are missing (cyan points) because of the smaller size considered in their study, that again influence the initial disk fraction and disk decay time.

The corresponding paper is currently under review and we are about to finish the referee report. So stay tuned for more in-depth discussion and additional analysis!

References:
[F10] Fedele, et al. 2010, A&A, 510, A72
[GC21] Gaia Collaboration, Brown, et al. 2021,A&A, 649, A1
[G19] Großschedl, et al. 2019, A&A, 622, A149
[KL14] Koenig & Leisawitz 2014, ApJ, 791, 131
[L22] Luhman 2022, AJ, 163, 25
[M21] Michel, et al. 2021, ApJ, 921, 72
[P22] Pfalzner, et al. 2022, ApJ, 939, L10
[R23a] Ratzenböck, et al. 2023, A&A, 677, A59
[R23b] Ratzenböck, et al. 2023, A&A, 678, A71
[R14] Ribas, et al. 2014, A&A, 561, A54
[R15] Ribas, et al. 2015, A&A, 576, A52
[R18] Richert, et al. 2018, MNRAS, 477, 5191

universität wien
institut für astrophysik
UNIVERSITÄTSSTERNWARTE WIEN